Solar Phys (2011) 273:393–402
DOI 10.1007/s11207-011-9794-6

Magnetoacoustic Wave Trains in the 11 July 2005 Radio Event with Fiber Bursts

H. Mészárosová · M. Karlický · J. Rybák

Received: 29 November 2010 / Accepted: 12 May 2011 / Published online: 1 July 2011

Abstract A dm-radio emission with fiber bursts observed on 11 July 2005 was analyzed using wavelet filtration and spectral methods. In filtered radio spectra we found structures with different characteristic period P and frequency drift FD: *i*) fiber substructures (composed of dot emissions) with $P_1 \approx 0.5$ s, $\mathrm{FD}_1 = -87$ MHz s^{-1} on average, *ii*) fiber structures with $P_2 \approx 1.9$ s, and *iii*) drifting structures with $P_3 \approx 81.4$ s, $\mathrm{FD}_2 = -8.7, +98.5$, and -21.8 MHz s^{-1}. In the wavelet spectra we recognized patterns having the form of tadpoles. They were detected with the same characteristic periods P as found for the filtered structures. The frequency drift of the tadpole heads is found to be equal to the frequency drift of some groups of fibers for the long-period wavelet tadpoles (P_3) and to the frequency drift of individual fibers for the short-period tadpoles (P_2). Considering these wavelet tadpoles as signatures of propagating magnetoacoustic wave trains, the results indicate the presence of several wave trains in the fibers' source. While the long-period wave trains trigger or modulate a whole group of fibers, the short-period ones look like being connected with individual fiber bursts. This result supports the model of fibers based on magnetoacoustic waves. Using a density model of the solar atmosphere we derived the velocities of the magnetoacoustic waves, 107 and 562 km s^{-1}, and setting them equal to the Alfvén ones we estimated the magnetic field in the source of fiber bursts as 10.7 and 47.8 G.

Keywords Sun: corona · Sun: flares · Sun: radio radiation · Sun: oscillations · Methods: data analysis

Energy Storage and Release through the Solar Activity Cycle–Models Meet Radio Observations
Guest Editors: Christophe Marqué and Alexander Nindos

H. Mészárosová (✉) · M. Karlický
Astronomical Institute, Academy of Sciences of the Czech Republic, 25165 Ondřejov, Czech Republic
e-mail: hana@asu.cas.cz

M. Karlický
e-mail: karlicky@asu.cas.cz

J. Rybák
Astronomical Institute, Slovak Academy of Sciences, 05960 Tatranská Lomnica, Slovak Republic
e-mail: rybak@astro.sk

1. Introduction

It was theoretically predicted by Roberts, Edwin, and Benz (1983, 1984) that impulsively generated signals (produced *e.g.* by solar flares) can generate propagating magnetoacoustic wave trains. These wave trains can be trapped in regions with higher density, *e.g.* in coronal loops. Nakariakov *et al.* (2004) studied these magnetoacoustic wave trains numerically. They showed that these trains in the wavelet spectrum correspond to the pattern where a narrowband tail precedes broadband head. Due to the shape of this pattern (tail plus head) they named these characteristic patterns wavelet tadpoles. (Please note here the tadpoles mean tadpoles in the wavelet spectra (Nakariakov *et al.*, 2004; Aschwanden, 2005), not the tadpole radio bursts (Kuijpers, 1975a; Slottje, 1981).) The wavelet tadpoles of the present type were observed in solar eclipse data (Katsiyannis *et al.*, 2003) and in decimetric radio bursts of both the gyrosychrotron (Mészárosová *et al.*, 2009a) and plasma emissions (Mészárosová *et al.*, 2009b).

Complex decimetric radio emissions are characterized by many radio bursts and fine structures (Jiřička *et al.*, 2001). Among them the fiber bursts (or fibers), which are considered to be a fine structure of type IV bursts, are defined as short-lasting and repeated bursts with a frequency drift of about $-100\,\mathrm{MHz\,s^{-1}}$. Individual fibers can even be composed of distinct (isolated) emission dots (for more details of these substructures, see Mészárosová *et al.*, 2008).

In the present paper we search for both the characteristic radio structures and the magnetoacoustic wave trains (tadpoles in the wavelet spectra) in complex radio spectrum. Analyzing these radio structures and wavelet tadpoles we want to contribute to a better understanding of fiber bursts.

The paper is organized as follows: in Section 2 we present the observations, in Section 3 the wavelet analysis of these data is described and in Section 4 we discuss our results and draw our conclusions.

2. Observations

The 11 July 2005 decimetric radio event (16:31:40 – 16:43:20 UT, 800 – 2000 MHz), associated with fiber bursts (Figure 1, upper panel), was recorded by the Ondřejov radio spectrograph (Jiřička *et al.*, 1993, time resolution = 0.1 s, frequency resolution = 5 MHz). This event classified as C1.1 (GOES X-ray maximum at 16:38 UT) was observed in the active region NOAA AR 10786 after the flare classified as C8.4 (GOES X-ray maximum at 15:08 UT, Hα importance SF).

The whole radio event consists of several groups of fiber bursts and underlying continua with a characteristic intensity of 180 – 700 SFU except for the time interval 16:35:45 – 16:36:17 UT with the characteristic intensity of 1080 – 2070 SFU. Individual groups of fibers have different global frequency drifts, as studied in detail in the following. The most remarkable property is the frequency drift of the individual fiber bursts that ranges from -71 to $-144\,\mathrm{MHz\,s^{-1}}$ ($-105\,\mathrm{MHz\,s^{-1}}$ on average). The fibers in the time interval 16:35:50 – 16:36:40 UT are shown in Figure 2 (upper panel). Most of these fibers are composed of emission dots (Mészárosová *et al.*, 2008).

The fibers with long-period wavelet tadpoles in time interval 16:38 – 16:41 UT were previously studied by Mészárosová *et al.* (2009b). Here, we extended our study to the whole radio event (16:31:40 – 16:43:20 UT); especially to its most complex part (16:35:50 – 16:36:40 UT). Furthermore, we extended also the range of periods studied to shorter ones.

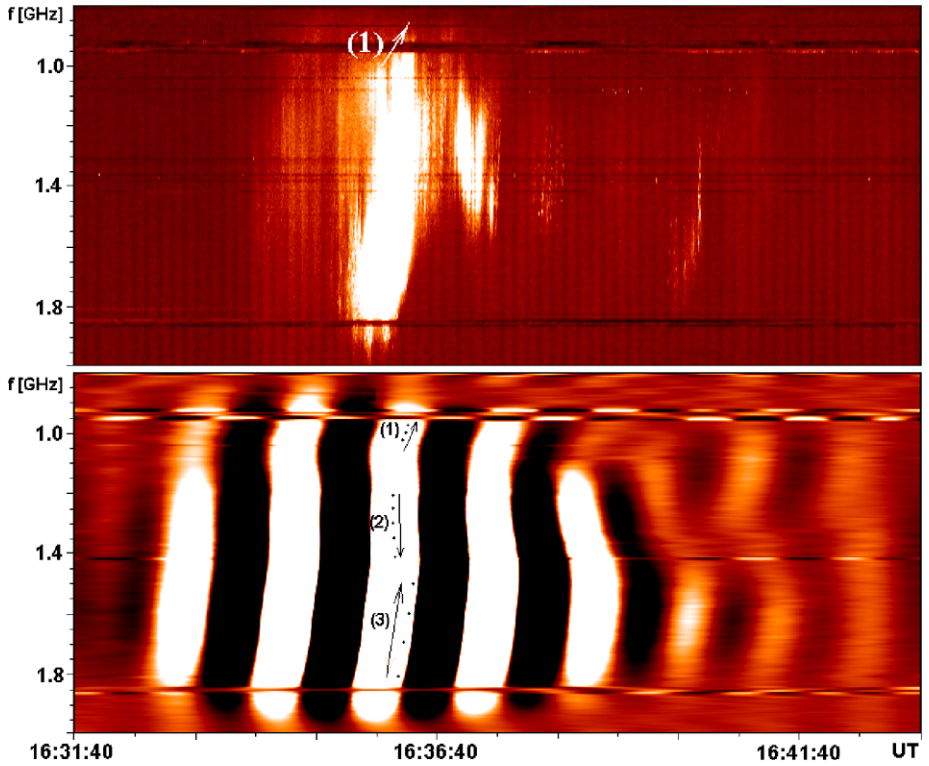

Figure 1 Upper panel: Global view on 11 July 2005 of the dm-radio event recorded by the Ondřejov radio spectrograph (16:31:40 – 16:43:20 UT, 800 – 2000 MHz), which consists of groups of fiber bursts and underlying continuum. Bottom panel: Filtered radio spectrum with the characteristic period $P = 81.4$ s showing structure with three different frequency drifts, marked by black arrows 1, 2, and 3 equal to -8.7, $+98.5$, and -21.8 MHz s^{-1}, respectively. The frequency drift (black arrow 1) is equal to the frequency drift (white arrow 1) in the upper panel. The individual black points indicate the individual wavelet tadpole head maxima in Figures 4 – 6.

3. Wavelet Analysis of the 11 July 2005 Radio Event with Fibers

To find the characteristic properties of the 11 July 2005 radio event with fibers we used two independent methods of wavelet analysis:

i) wavelet time filtration of a complex radio spectrum to separate individual drifting structures which are present in the original complex radio dynamic spectrum;
ii) wavelet power spectra of radio flux time series at individual frequencies to detect characteristic wavelet tadpole patterns as signatures of magnetoacoustic wave trains.

We focused on characteristic periods and frequency drifts of both the separated structures and the corresponding magnetoacoustic wave trains to find possible relations between them.

3.1. Wavelet Time Separation of Drifting Structures in a Complex Radio Spectrum

We used a new method of the separation of drifting structures in a complex radio spectrum developed by Mészárosová, Rybák, and Karlický (2011). It gives us two independent possibilities on how to separate individual structures (bursts) of the original radio spectrum;

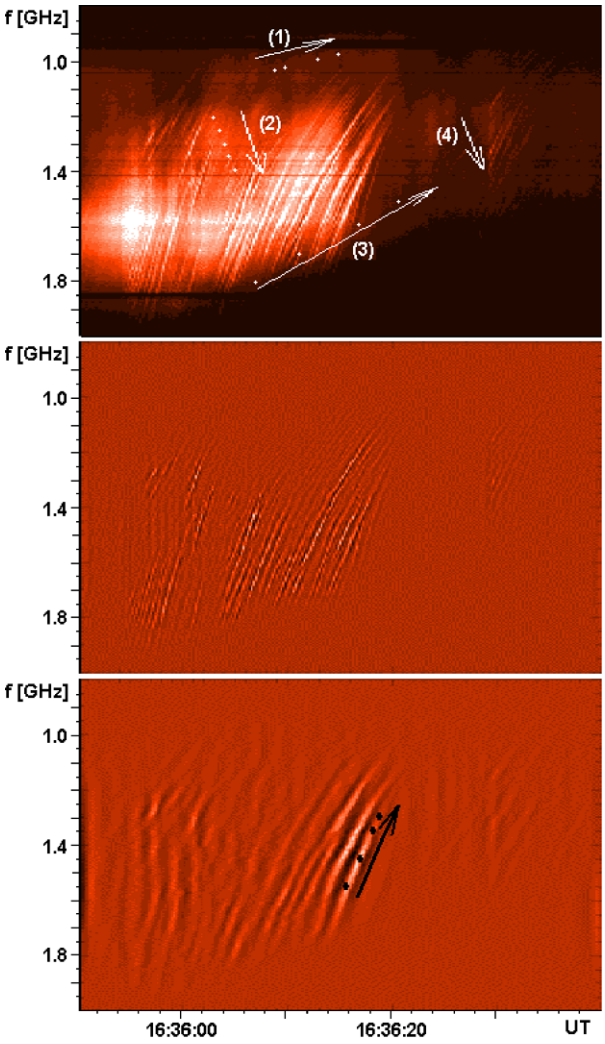

Figure 2 Upper panel: Detailed view on fiber bursts in the time interval 16:35:50 – 16:36:40 UT. The frequency drifts (arrows 1 – 3) equal the frequency drifts obtained by the wavelet method and the individual white points indicate individual wavelet tadpole head maxima in Figures 4 – 6. The frequency drift (arrow 4) equals that of arrow 2. Middle panel: Filtered radio spectrum with the characteristic period $P \approx 0.5$ s showing the fiber substructures (composed of dot emissions) with characteristic frequency drift -87 MHz s^{-1} on average. Bottom panel: Filtered radio spectrum with the characteristic period $P \approx 1.9$ s showing fiber structures with characteristic frequency drift -78 MHz s^{-1} on average (black arrow). The individual black points indicate the individual wavelet tadpole head maxima at four selected frequencies.

in time and in frequency. Here, we used the time separation, *i.e.* separation according to characteristic period(s) of the individual structures.

Only one characteristic period $P = 81.4$ s was found to be present at all frequencies during the whole event (16:31:40 – 16:43:20 UT, upper panel in Figure 1). This period P was found in the period range 70 – 90 s, which was determined from the averaged global wavelet spectrum (for more details, see Section 2 in Mészárosová, Rybák, and Karlický, 2011). The filtered radio spectrum is presented in the bottom panel of Figure 1. At least three different frequency drifts in this radio structure were found (black arrows 1, 2, and 3), which are equal to -8.7, $+98.5$, and -21.8 MHz s^{-1} at frequency ranges about 800 – 1050, 1050 – 1450, 1450 – 2000 MHz, respectively.

Two characteristic periods $P \approx 0.5$ s (computed in the period range 0.3 – 1.0 s) and $P \approx 1.9$ s (computed in the period range 1.0 – 3.0 s) were found to be present during the selected time interval 16:35:50 – 16:36:40 UT (Figure 2, upper panel). The filtered radio spectrum with the characteristic periods $P \approx 0.5$ s is shown in the middle panel of Figure 2.

It presents fiber substructures composed of emission dots. Their frequency drift is -70 down to -100 MHz s^{-1} (-87 MHz s^{-1} on average). In addition, the filtered radio spectrum with the characteristic periods $P \approx 1.9$ s is presented in the bottom panel of Figure 2. It consist of fiber structures with frequency drifts ranging from -60 to -100 MHz s^{-1} (-78 MHz s^{-1} on average; see also the black arrow, bottom panel).

Thus, the original complex radio spectrum consists of at least three different radio structures.

3.2. Wavelet Power Spectra with Tadpole Patterns

We searched for the wavelet power spectra with tadpole patterns as signatures of the magnetoacoustic wave trains (Nakariakov *et al.*, 2004). We used the wavelet analysis method (Torrence and Compo, 1998) with the Morlet mother function. In these wavelet spectra we determined the characteristic periods of wavelet tadpole patterns, the cone of influence COI (hatched regions where edge effects become important due to finite-length time series) and the confidence level CL (relative to red noise). Only the regions outside the COI with CL above 90% were considered as significant in each time series. The spectra are plotted with the lighter areas indicating greater power.

The original radio spectra, shown in Figure 1 and 2 (upper panels), were divided into 256 radio flux time series at individual frequencies (cuts of the radio spectrum along time) from 800 to 2000 MHz. As a result of this analysis, we found the wavelet tadpole patterns with characteristic periods $P \approx 0.5$ s, $P \approx 1.9$ s and $P = 81.4$ s during time intervals 16:35:50 – 16:36:20, 16:36:10 – 16:36:20, and 16:33:30 – 16:38:20 UT, respectively. Thus, individual wavelet tadpoles have the same characteristic period P as the individual separated radio structures. We search for frequency drifts of the wavelet tadpole head maxima, similarly as in the paper by Mészárosová *et al.* (2009b).

The maxima of wavelet tadpole heads with characteristic period $P \approx 0.5$ s are present rather chaotically during the time interval 16:35:50 – 16:36:20 UT, *i.e.* without a significant frequency drift. A typical example of such a wavelet tadpole as a signature of the magnetoacoustic wave train (plot period *vs.* time) detected at the radio frequency 1391 MHz is shown in Figure 3 (upper panel).

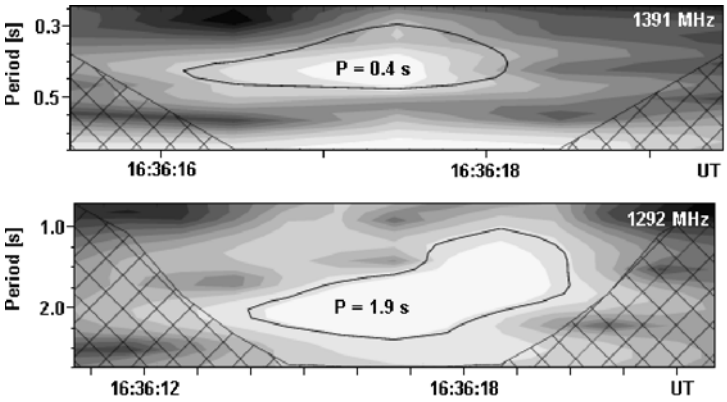

Figure 3 Upper panel: Example of the wavelet power spectrum with the wavelet tadpole pattern and the characteristic period $P = 0.4$ s. Bottom panel: Example of the wavelet power spectrum with the wavelet tadpole pattern and the characteristic period $P = 1.9$ s.

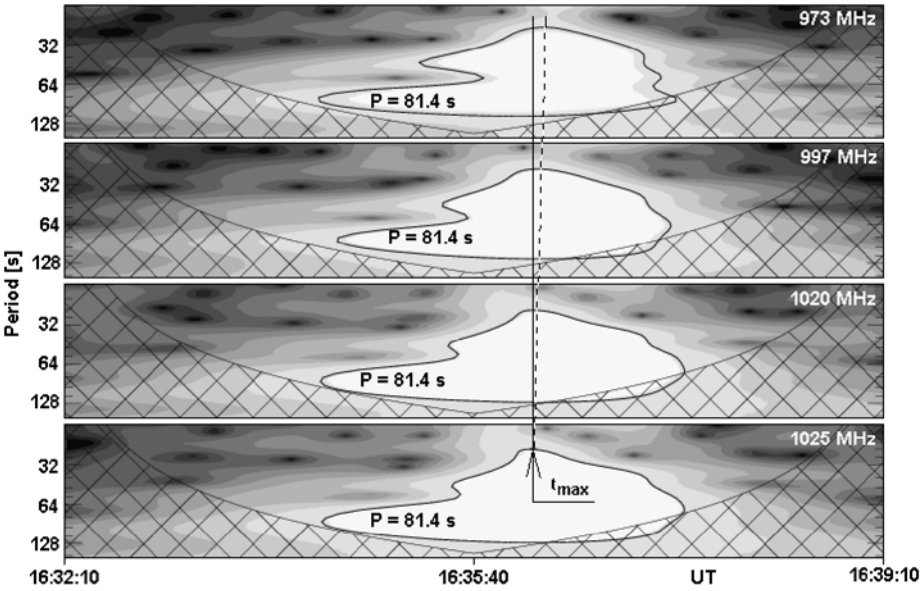

Figure 4 Wavelet tadpoles as signatures of a magnetoacoustic wave train in the 973 – 1025 MHz frequency range. The panels show wavelet power spectra with tadpole patterns and the characteristic period of $P = 81.4$ s. The solid line represents time t_{max} of the tadpole head maximum at the highest frequency and the dashed line shows the negative frequency drift of these head maxima toward lower frequencies (-8.7 MHz s^{-1}; see also arrow 1 in Figure 1).

A typical example of a wavelet tadpole with characteristic period $P \approx 1.9$ s detected at the radio frequency 1292 MHz is shown in the bottom panel (Figure 3). The black points (Figure 2, bottom panel) indicate the time of wavelet tadpole head maxima at four selected frequencies (1292, 1348, 1447, and 1555 MHz). Here, we can see that these maxima show a similar frequency drift as fibers.

Typical examples of the wavelet tadpoles with the period $P = 81.4$ s are shown in Figures 4 – 6. The panels show wavelet power spectra detected at selected radio frequencies. The solid line represents the wavelet tadpole head maximum at the highest frequency and the frequency drift of the heads of individual wavelet tadpoles is indicated by the dashed line.

For these long-period wavelet tadpoles we found three different frequency drifts of wavelet tadpole head maxima. The wavelet tadpoles in Figures 4 and 6 drift toward higher frequencies with the negative frequency drifts -8.7 and -21.8 MHz s^{-1}, respectively. Wavelet tadpoles in Figure 5 drift toward lower frequencies with a positive frequency drift $+98.5$ MHz s^{-1}.

We studied relations between wavelet tadpole head maxima with a period of $P = 81.4$ s and the separated radio structures with the same characteristic period. In the bottom panel (Figure 1) the black points indicate the time of wavelet tadpole head maxima at the same selected frequencies as in Figures 4 – 6. We can see that these maxima show a similar frequency drift to that of the filtered structures (black arrows 1 – 3). These maxima were found at times of the highest intensity of the whole radio event.

Furthermore, these drifts can also be seen in the original radio dynamic spectrum. The negative frequency drifts -8.7 and -21.8 MHz s^{-1} are shown at the upper panel of Figure 2 (white arrow 1 and 3), respectively. The first one is also detected at the upper panel of

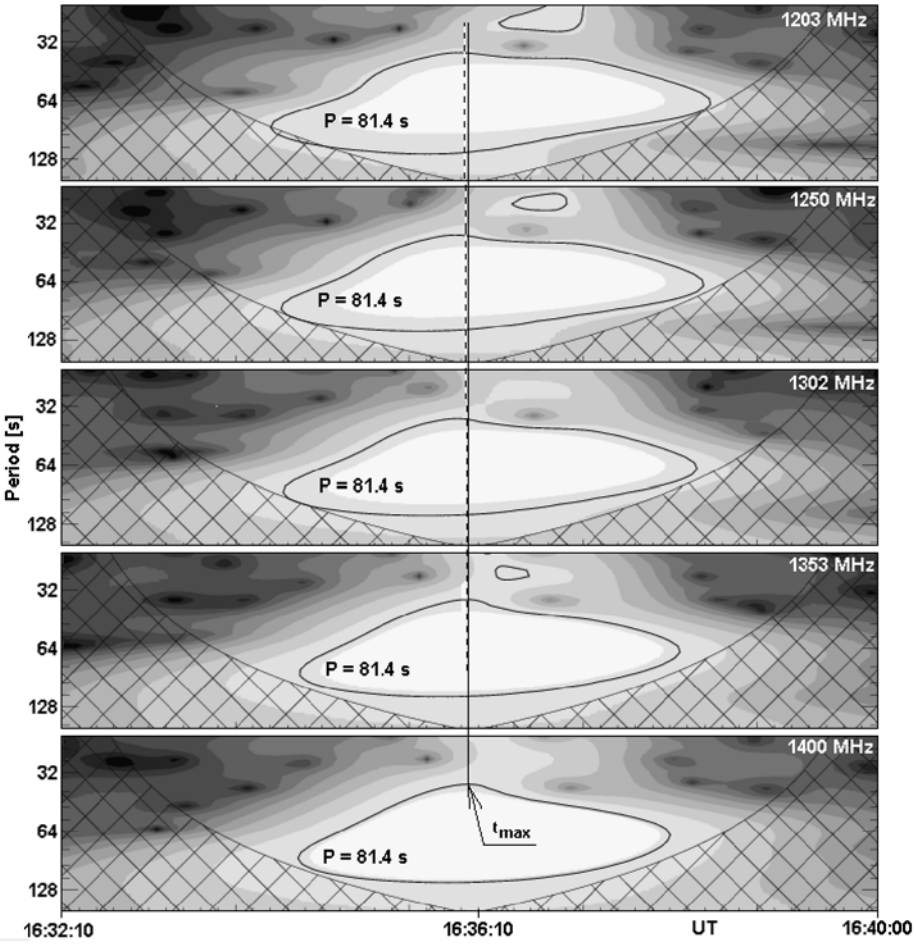

Figure 5 Wavelet tadpoles as signatures of the magnetoacoustic wave train in the 1203 – 1400 MHz frequency range. The panels show wavelet power spectra with tadpole patterns and the characteristic period $P = 81.4$ s. The solid line represents time $t_{\max}$ of the head tadpole maximum at the highest frequency and the dashed line shows the positive frequency drift of these head maxima toward higher frequencies ($+98.5$ MHz s^{-1}; see also arrow 2 in Figure 1, bottom panel).

Figure 1 (arrow 1). The positive frequency drift ($+98.5$ MHz s^{-1}) is shown in the upper panel of Figure 2 (white arrows 2 and 4). The white points (upper panel of Figure 1) indicate the wavelet tadpoles head maxima at selected frequencies in Figures 4 – 6. It is remarkable that the times of the wavelet tadpole head maxima (arrow 3 in Figure 2) correspond to the starting times of fiber bursts. This result is the same as in our previous study of fiber bursts in the interval 16:38 – 16:41 UT (Mészárosová *et al.*, 2009b). The other arrows (1 and 2) do not show such a correspondence. Nevertheless, the drift of arrow 2 is the same as that of starting frequencies of the fibers designated by the arrow 4.

Thus, we found that all three frequency drifts of wavelet tadpoles head maxima with the characteristic period $P = 81.4$ s (Figures 4 – 6) are similar to the ones of separated radio structures (Figure 1, bottom panel) and they correspond to global frequency drifts of the groups of fibers in the original radio spectrum (upper panels in Figures 1 and 2).

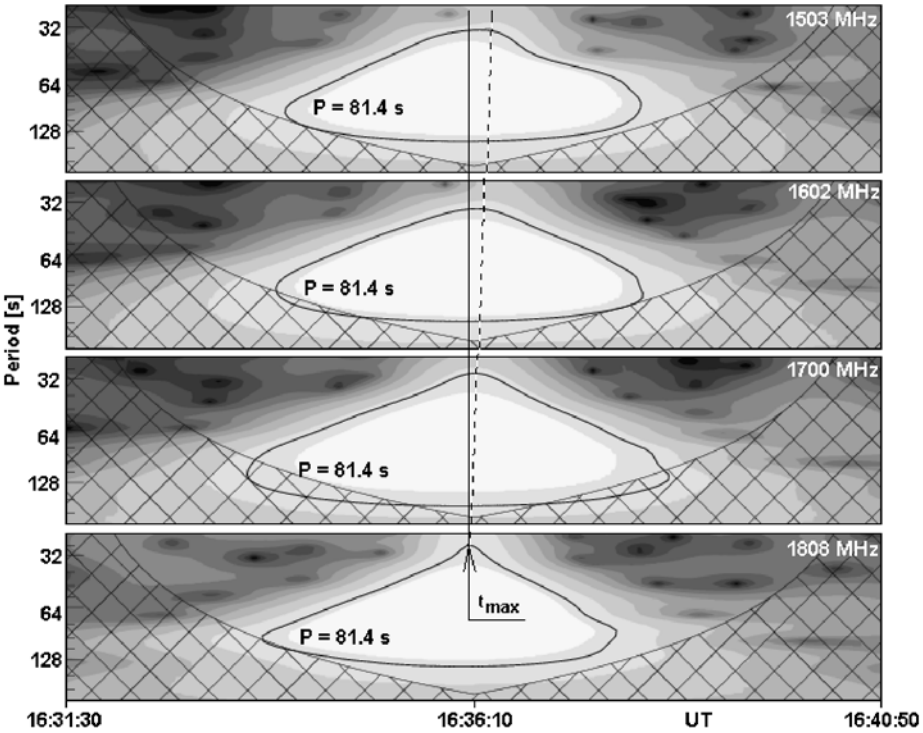

Figure 6 Wavelet tadpoles as signatures of the magnetoacoustic wave train in the 1503 – 1808 MHz frequency range. The panels show wavelet power spectra with tadpole patterns and the characteristic period $P = 81.4$ s. The solid line represents the time t_{max} of the head tadpole maximum at the highest frequency and the dashed line shows the negative frequency drift of these head maxima toward lower frequencies (-21.8 MHz s^{-1}; see also arrow 3 in Figure 1, bottom panel).

4. Discussion and Conclusions

We have found that the complex radio spectrum observed on 11 July 2005 (upper panels in Figures 1 and 2) consists of at least three different radio structures (middle and bottom panels in Figures 1 and 2) with different characteristic periods. We have also detected the presence of tadpole wavelet patterns; see Figures 3 – 6 with the same characteristic periods as found for the separated (filtered) radio structures. Furthermore, we found that the maxima of the wavelet tadpole heads for the period $P = 81.4$ s were located at the upper frequency boundary of a group of fibers, and the maxima of the tadpole heads for the period $P \approx 1.9$ s drifted along one strong fiber.

We interpret these wavelet tadpole patterns of radio emission fluxes as signatures of magnetoacoustic wave trains in accordance with the papers of Katsiyannis *et al.* (2003), Nakariakov *et al.* (2004), and Mészárosová *et al.* (2009a, 2009b). It means that in the radio source of fibers there are at least three types of magnetoacoustic wave trains. While the long-period wave train (with $P = 81.4$ s) triggers or modulates a whole group of fiber bursts, the short-period one (with $P \approx 1.9$ s) looks like being connected with individual fiber bursts.

Let us discuss these results in the frame of existing models of fiber bursts. Generally, these models can be divided into three groups:

Table 1 Parameters of the long-period (case 3) and short-period magnetoacoustic waves (t_{max} = time of wavelet tadpole head maximum, FD = frequency drift of head maxima, n_e = average electron density, h = mean coronal altitudes, v = wave train velocity, B = magnetic field strength).

Period (s)	Frequency (MHz)	t_{max} (UT)	FD (MHz s^{-1})	n_e (cm^{-3})	h (Mm)	v (km s^{-1})	B (G)
81.4	1503	16:36:21		2.80×10^{10}	10.5		
	1808	16:36:07	−21.8	4.05×10^{10}	8.9	107	10.7
1.9	1292	16:36:19		2.07×10^{10}	11.9		
	1550	16:36:16	−86	2.98×10^{10}	10.2	562	47.8

i) models based on whistler waves (Kuijpers, 1975b; Mann, Karlický, and Motschmann, 1987; Mann *et al.*, 1989),
ii) models considering nonlinear Alfvén solitons (Bernold and Treumann, 1983; Treumann, Güdel, and Benz, 1990), and
iii) models with sausage magnetoacoustic waves (Kuznetsov, 2006).

These models were proposed for the generation of individual fibers. In our case, we found that one fiber drifted simultaneously with the signature of the magnetoacoustic wave train (maxima of the wavelet tadpoles). This fact agrees only with the model of fibers by Kuznetsov (2006). It is a very interesting result; however, it needs to be taken with caution, because it was found by a complex method, and up to now only in the present case. Therefore, further verification of this result for more events is necessary. As regards the long-period ($P = 81.4$ s) magnetoacoustic wave train, which was also present in the source of fibers, it can be considered as the one modulating or triggering the whole group of fibers.

Now, without consideration of any specific fiber bursts model, the frequency drifts of the heads of the magnetoacoustic wave trains can be used for the estimation of the magnetic field.

Let us consider two cases, the long-period magnetoacoustic wave train (case 3, in Figure 2, upper panel) and short-period train (Figure 2, bottom panel). While in the first case the head maxima follow the starting frequencies of the fibers, in the second case the head maxima correspond to the shape of fibers. We assume that the magnetoacoustic wave trains move upwards in the density stratified atmosphere and modulate the radio emission produced by plasma emission mechanism at the plasma frequency. Then using the density model of the solar atmosphere by Aschwanden (2002), we derive the velocities of these wave trains as 107 and 562 km s^{-1} (Table 1). The maximum amplitude of these trains corresponds to the head maximum of the wavelet tadpoles (Nakariakov *et al.*, 2004). Furthermore, at times of the head maximum of wavelet tadpoles, the group velocity of the corresponding magnetoacoustic wave train is close to the Alfvén velocity inside the guiding loop (Roberts, Edwin, and Benz, 1984). Thus, setting these velocities equal to the Alfvén ones we estimated the magnetic field in the mentioned two cases as 10.7 and 47.8 G (Table 1). Furthermore, we can estimate the width of the density structures (loops) in the solar atmosphere guiding these two magnetoacoustic trains as (width $\sim$ period times wave train velocity) 8700 and 1070 km. Because the long-period wave train influences the short-period one, *e.g.* through triggering and modulation of fibers, it indicates that the narrower guiding structure is probably inside or close to the broader one.

Acknowledgements H.M. and M.K. acknowledge support from the Grant IAA300030701 of the Academy of Sciences of the Czech Republic and the research project AVOZ10030501 of the Astronomical Institute AS

CR. The work of J.R. was partly supported by the Slovak Grant Agency VEGA (project 2/0064/09). The program of mobility between the academies of the Czech Republic and Slovakia is also acknowledged. The wavelet analysis was performed using the software based on tools provided by C. Torrence and G.P. Compo at http://paos.colorado.edu/research/wavelets.

References

Aschwanden, M.J.: 2002, *Space Sci. Rev.* **101**, 1.
Aschwanden, M.J.: 2005, In: *Physics of the Solar Corona*, Praxis, Chichester.
Bernold, T., Treumann, R.: 1983, *Astrophys. J.* **264**, 677.
Jiřička, K., Karlický, M., Kepka, O., Tlamicha, A.: 1993, *Solar Phys.* **147**, 203.
Jiřička, K., Karlický, M., Mészárosová, H., Snížek, V.: 2001, *Astron. Astrophys.* **375**, 243.
Katsiyannis, A.C., Williams, D.R., McAteer, R.T.J., Gallagher, P.T., Keenan, F.P., Murtagh, F.: 2003, *Astron. Astrophys.* **406**, 709.
Kuijpers, J.: 1975a, In: *Doctor in de Wiskunde en Natuurwetenschappen Dissertation*, Rijksuniversiteit, Utrecht.
Kuijpers, J.: 1975b, *Solar Phys.* **44**, 173.
Kuznetsov, A.A.: 2006, *Solar Phys.* **237**, 153.
Mann, G., Karlický, M., Motschmann, U.: 1987, *Solar Phys.* **110**, 381.
Mann, G., Baumgartel, K., Chernov, G., Karlický, M.: 1989, *Solar Phys.* **120**, 383.
Mészárosová, H., Rybák, J., Karlický, M.: 2011, *Astron. Astrophys.* **525**, A88.
Mészárosová, H., Karlický, M., Sawant, H.S., Fernandes, F.C.R., Cecatto, J.R., de Andrade, M.C.: 2008, *Astron. Astrophys.* **491**, 555.
Mészárosová, H., Karlický, M., Rybák, J., Jiřička, K.: 2009a, *Astrophys. J. Lett.* **697**, L108.
Mészárosová, H., Karlický, M., Rybák, J., Jiřička, K.: 2009b, *Astron. Astrophys.* **502**, L13.
Nakariakov, V.M., Arber, T.D., Ault, C.E., Katsiyannis, A.C., Williams, D.R., Keenan, F.P.: 2004, *Mon. Not. Roy. Astron. Soc.* **349**, 705.
Roberts, B., Edwin, P.M., Benz, A.O.: 1983, *Nature* **305**, 688.
Roberts, B., Edwin, P.M., Benz, A.O.: 1984, *Astrophys. J.* **279**, 857.
Slottje, C.: 1981, In: *Atlas of Fine Structures of Dynamic Spectra of Solar Type IV-dm and Some Type II Radio Bursts*, Netherlands Foundation for Radio Astronomy, Dwingeloo.
Torrence, C., Compo, G.P.: 1998, *Bull. Am. Meteorol. Soc.* **79**, 61.
Treumann, R., Güdel, M., Benz, A.O.: 1990, *Astron. Astrophys.* **236**, 242.